A&A 495, 359–362 (2009)
DOI: 10.1051/0004-6361:200811222

Astronomy & Astrophysics

Ultraviolet and extreme-ultraviolet line ratio diagnostics for O IV

F. P. Keenan, P. J. Crockett, K. M. Aggarwal, D. B. Jess, and M. Mathioudakis

Astrophysics Research Centre, School of Mathematics and Physics, Queen's University Belfast, Belfast BT7 1NN, Northern Ireland, UK
e-mail: F.Keenan@qub.ac.uk

Received 24 October 2008 / Accepted 18 December 2008

ABSTRACT

Aims. We generate theoretical ultraviolet and extreme-ultraviolet emission line ratios for O IV and show their strong versatility as electron temperature and density diagnostics for astrophysical plasmas.
Methods. Recent fully relativistic calculations of radiative rates and electron impact excitation cross sections for O IV, supplemented with earlier data for *A*-values and proton excitation rates, are used to derive theoretical O IV line intensity ratios for a wide range of electron temperatures and densities.
Results. Diagnostic line ratios involving ultraviolet or extreme-ultraviolet transitions in O IV are presented, that are applicable to a wide variety of astrophysical plasmas ranging from low density gaseous nebulae to the densest solar and stellar flares. Comparisons with observational data, where available, show good agreement between theory and experiment, providing support for the accuracy of the diagnostics. However, diagnostics are also presented involving lines that are blended in existing astronomical spectra, in the hope this might encourage further observational studies at higher spectral resolution.

Key words. atomic processes – Sun: UV radiation – planetary nebulae: general – ultraviolet: general

1. Introduction

Ultraviolet and extreme-ultraviolet emission lines arising from transitions in B-like O IV are detected from a wide variety of astronomical sources, ranging from the Sun (Sandlin et al. 1986) to other stars (Christian et al. 2004), gaseous nebulae (Feibelman 1997) and supernova remnants (Blair et al. 1991). The diagnostic potential of these lines to provide electron temperature (T_e) and density (N_e) diagnostics for the emitting plasma was first shown by Flower & Nussbaumer (1975), who also calculated radiative rates plus electron and proton impact excitation cross sections for the ion. Since then, many authors have generated atomic data for O IV that have subsequently been used to derive theoretical diagnostic line ratios (see Tayal 2006, and references therein).

Very recently, Aggarwal & Keenan (2008) have employed the fully relativistic GRASP and Dirac RMATRX codes to calculate radiative rates and electron impact excitation cross sections, respectively, for all transitions among the energetically lowest 75 fine-structure levels of O IV. These results are the most extensive currently available for O IV, and also should be the most reliable, at least for the excitation cross sections, as discussed in detail by Aggarwal & Keenan. In this paper we use these data, supplemented with previous highly accurate calculations for radiative rates and proton excitation cross sections, to derive theoretical O IV ultraviolet and extreme-ultraviolet emission line ratios applicable to a wide range of astrophysical plasmas. We demonstrate the versatility of O IV plasma diagnostics, which can provide temperature and density estimates for a wide variety of astronomical sources ranging from low density gaseous nebulae up to the densest solar and stellar flares.

2. Atomic data and theoretical line ratios

The model ion for O IV consisted of the 75 fine-structure levels arising from the $2s^22p$, $2s2p^2$, $2p^3$, $2s^23\ell$ (ℓ = s, p, d), $2s2p3\ell$ (ℓ = s, p, d) and $2s^24\ell$ (ℓ = s, p, d, f) configurations. Energies for all these levels were obtained from the compilation of experimental values by the National Institute of Standards and Technology, which may be found at their website http://physics.nist.gov/PhysRefData/. Test calculations including additional levels, such as those arising from the $2s^25\ell$ and $2s2p4\ell$ configurations, were found to have a negligible effect on the theoretical line ratios considered in the present paper.

Einstein *A*-coefficients for transitions in O IV were obtained from the following sources: (i) Galavís et al. (1998) for the forbidden $2s^22p\ ^2P_{1/2}$–$2s^22p\ ^2P_{3/2}$ transition; (ii) Corrégé & Hibbert (2002) for the $2s^22p\ ^2P_J$–$2s2p^2\ ^4P_{J'}$ intercombination lines; (iii) Corrégé & Hibbert (2004) for allowed and intercombination lines among the $2s^22p$, $2s2p^2$, $2p^3$ and $2s^23\ell$ (ℓ = s, p, d) levels; (iv) Aggarwal & Keenan (2008) for all remaining transitions. For electron impact excitation rates, we have adopted the results of Aggarwal & Keenan, which contain several improvements over previous calculations for O IV undertaken with the RMATRX code (Zhang et al. 1994; Tayal 2006), including the greatest number of levels and the largest range of partial waves. They are hence probably the most accurate currently available for this ion, as discussed in detail by Aggarwal & Keenan. However, there is also scope for improvement, mainly due to the fact that the wavefunctions adopted in the calculations of Aggarwal & Keenan are not as accurate as those of some other workers, such as Tachiev & Froese-Fischer (2000) and Corrégé & Hibbert (2002). Indeed, this is why we have adopted the *A*-values of Corrégé & Hibbert (2002, 2004) where possible, as their results have an estimated uncertainty of only ±5%, compared to ±20% for those of Aggarwal & Keenan. The limitations in the wavefunctions of Aggarwal & Keenan may directly affect the subsequent determination of excitation rates, both for allowed and forbidden transitions. This is because for the weak allowed transitions, the *A*-values of Aggarwal & Keenan differ by up to 50% with those of Tachiev & Froese-Fischer (2000)

and Corrégé & Hibbert (2004), while some of the energy levels show discrepancies of up to 8% with the experimental values (see Tables 1 and 2 of Aggarwal & Keenan). Nevertheless, the estimated accuracy of the Aggarwal & Keenan excitation rate data is ±20% for a majority of transitions, and should be the most reliable currently available for O IV.

As noted by, for example, Seaton (1964), excitation by protons will be important for the $2s^22p\ ^2P_{1/2}$–$2s^22p\ ^2P_{3/2}$ transition, and in the present analysis we have used the theoretical results of Foster et al. (1996). However, Flower & Nussbaumer (1975) have pointed out that proton excitation should also be included for the $2s2p^2\ ^4P_J$–$2s2p^2\ ^4P_{J'}$ transitions in B-like ions, and for these rates we have adopted the calculations of Foster et al. (1997). Both the Foster et al. (1996, 1997) data are estimated to be accurate to ±10%.

Using the above atomic data in conjunction with a recently updated version of the statistical equilibrium code of Dufton (1977), relative O IV level populations and hence emission line strengths were calculated for two grids of electron temperature (T_e) and density (N_e) values. The first grid (for T_e = 10 000, 15 000, 20 000 and 30 000 K; $N_e = 10^2$–10^6 cm^{-3} in steps of 0.1 dex) is appropriate to nebular plasmas, while the second ($T_e = 10^{4.8}$–$10^{5.6}$ K in steps of 0.1 dex; $N_e = 10^8$–10^{14} cm^{-3} in steps of 0.1 dex) is for solar/stellar plasma conditions. In particular, the adopted temperature range for the latter covers that over which O IV has a fractional abundance in ionization equilibrium of N(O IV/N(O) ≥ 0.006 (Bryans et al. 2009), and hence should be appropriate to most coronal-type plasmas. Our results are too extensive to reproduce here, as with 75 fine-structure levels in our calculations we have intensities for 2775 transitions at each of the 530 possible (T_e, N_e) combinations considered. However, results involving any line pair, in either photon or energy units, are freely available from one of the authors (FPK) by email on request. Given errors in the adopted atomic data of between ±5% and ±20% (see above), we would expect our theoretical ratios to be accurate to better than ±15%.

3. Results and discussion

The O IV intercombination multiplet around 1400 Å provides excellent electron density diagnostics for both nebular and solar plasmas, as shown in Figs. 1–4, where we plot the emission line ratios R_1 = I(1407.3 Å)/I(1401.1 Å), R_2 = I(1404.7 Å)/I(1401.1 Å) and R_3 = I(1407.3 Å)/I(1404.7 Å) as a function of T_e and N_e. The transitions corresponding to these lines are listed in Table 1, as are those for the other O IV features discussed in this paper. We note that the ratios R_4 = I(1399.7 Å)/I(1401.1 Å) and R_5 = I(1397.2 Å)/I(1401.1 Å) have the same T_e and N_e dependence as R_1 and R_2, respectively (due to common upper levels), but with $R_4 = 1.02 \times R_1$ and $R_5 = 0.130 \times R_2$.

The above theoretical ratios are in good agreement with observations for gaseous nebulae, such as those by Keenan et al. (1993). For example, for the planetary nebula NGC 7662, Keenan et al. measured R_1 = 0.30, R_2 = 0.69 and R_4 = 0.29, implying electron densities of log N_e = 3.5, 4.0 and 3.5, respectively, from Figs. 1 and 2. These values are consistent, and also in agreement with the electron densities derived for NGC 7662 from line ratios in species with similar ionization potentials and hence spatial distributions to O IV, such as I(4711 Å)/I(4740 Å) in Ar IV and I(2424 Å)/I(2422 Å) in Ne IV, both of which indicate log N_e = 3.5 (Keenan et al. 1997, 1998). In addition, we note that Keenan et al. (2002) have measured O IV line ratios

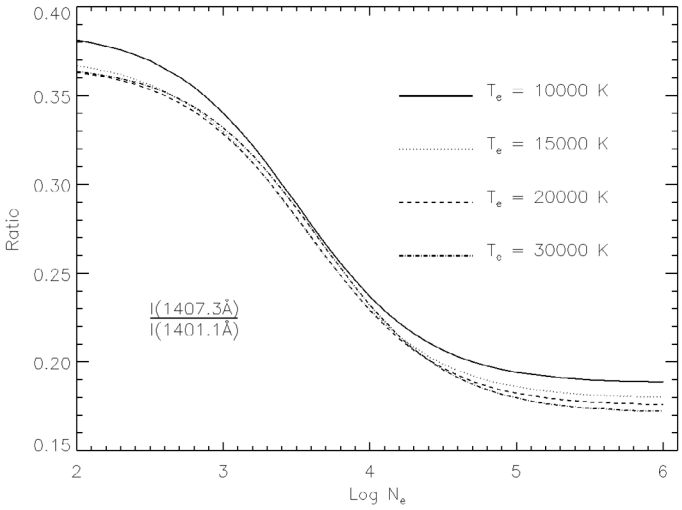

Fig. 1. The I(1407.3 Å)/I(1401.1 Å) line intensity ratio in O IV, where I is in energy units, plotted as a function of logarithmic electron density (N_e in cm^{-3}) at electron temperatures of T_e = 10 000, 15 000, 20 000 and 30 000 K.

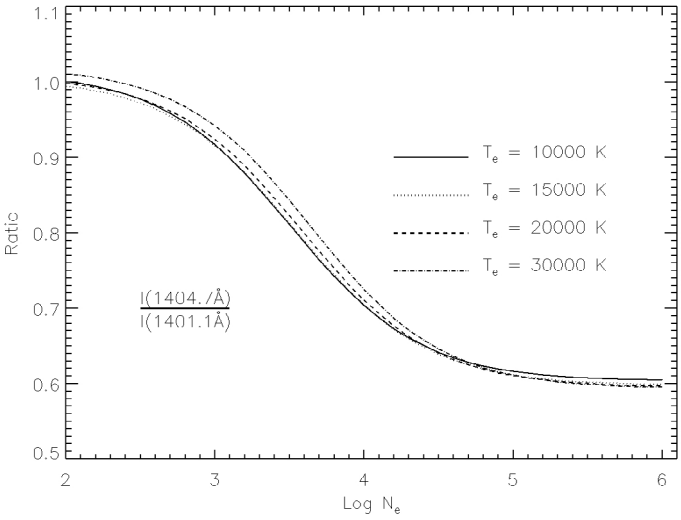

Fig. 2. Same as Fig. 1, but for the I(1404.7 Å)/I(1401.1 Å) ratio.

for the symbiotic star RR Tel. The diagnostic ratios for other species in the RR Tel spectrum, ranging from Al II to O V, indicate log $N_e \simeq 5$–8 (see Keenan et al. 2002, and references therein), over which density interval the theoretical values of R_1 through R_5 are predicted to be effectively constant (see Figs. 1 and 2). Once again, there is excellent agreement between theory and observation, with measured and predicted values of (theory in brackets) R_1 = 0.16 ± 0.02 (0.18), R_2 = 0.54 ± 0.05 (0.60), R_4 = 0.17 ± 0.02 (0.18) and R_5 = 0.077 ± 0.008 (0.077).

In existing solar spectra, such as those from the HRTS and SOHO/SUMER instruments, the O IV 1404.7 Å line is significantly blended with S IV (Brage et al. 1996; Keenan et al. 2002), although we note that the blending is negligible under nebular plasma conditions (Keenan et al. 2002). Additionally, the 1397.2 Å feature is very weak in solar spectra, and possibly blended, and hence its intensity should usually be considered an upper limit (Brage et al. 1996). However, the remaining useable density diagnostic line ratios R_1 and R_4 do provide consistent derivations of N_e. For example, for Active Region B at +2″ relative to the limb, Feldman & Doschek (1978) measured R_1 = 0.20

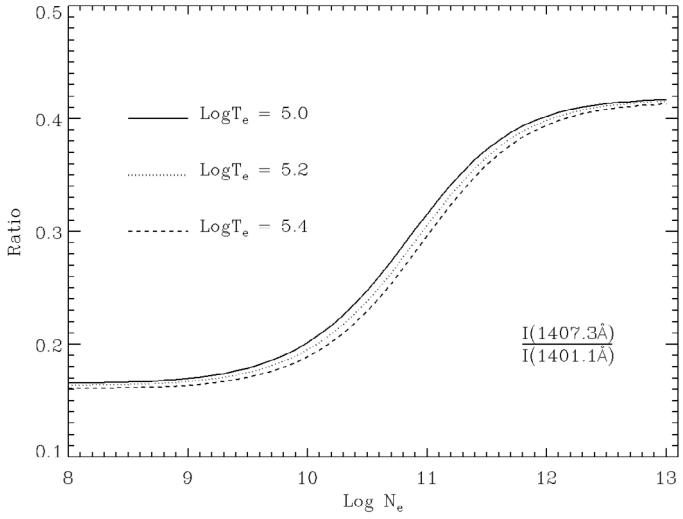

Fig. 3. The I(1407.3 Å)/I(1401.1 Å) line intensity ratio in O IV, where I is in energy units, plotted as a function of logarithmic electron density (N_e in cm^{-3}) at the electron temperature of maximum O IV fractional abundance in ionization equilibrium, $T_e = 10^{5.2}$ K (Bryans et al. 2009), plus ±0.2 dex about this value.

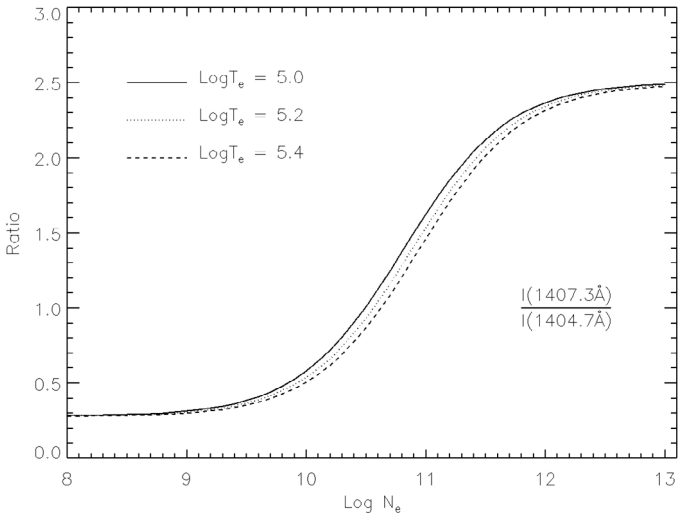

Fig. 4. Same as Fig. 3, but for the I(1407.3 Å)/I(1404.7 Å) ratio.

and $R_4 = 0.19$ from Skylab/S082A spectra, which both imply log $N_e = 10.1$ from Fig. 3, in good agreement with the value of log $N_e = 10.2$ found from line ratios in N IV, which is formed at the same temperature as O IV (Keenan et al. 1994).

The intercombination line ratios in O IV only provide useful electron density diagnostics for values of N_e up to about 10^{12} cm^{-3} (see Figs. 3 and 4). However, Kastner & Bhatia (1984) have pointed out that the allowed lines of O IV arising from 2s2p^2 ^{2}P–2p^3 ^{2}D transitions lie only ~60 Å from the intercombination multiplet, and their intensity ratios are very sensitive to the electron density for $N_e > 10^{11}$ cm^{-3}. They hence should provide good N_e-diagnostics for very high density astronomical plasmas such as solar and stellar flares. In Fig. 5 we plot the ratio $R_6 = I$(1343.5 Å)/I(1407.3 Å) as a function of both T_e and N_e, as the 1343.5 Å transition is the only line in the 2s2p^2 ^{2}P–2p^3 ^{2}D multiplet which is unblended in existing solar spectra (Cook et al. 1994). The measured values of $R_6 = 0.89$ and 0.90 for the flares of 1973 August 9 and 1973 September 7, from Skylab/S082B spectra (Cook et al. 1994), both indicate

Table 1. Summary of O IV transitions.

Wavelength (Å)	Transition
554.51	2s^{2}2p ^{2}P$_{3/2}$–2s2p^2 ^{2}P$_{3/2}$
625.85	2s2p^2 ^{4}P$_{5/2}$–2p^3 ^{4}S$_{3/2}$
779.91	2s2p^2 ^{2}D$_{5/2}$–2p^3 ^{2}D$_{5/2}$
787.71	2s^{2}2p ^{2}P$_{1/2}$–2s2p^2 ^{2}D$_{3/2}$
790.20	2s^{2}2p ^{2}P$_{3/2}$–2s2p^2 ^{2}D$_{5/2}$
1343.5	2s2p^2 ^{2}P$_{3/2}$–2p^3 ^{2}D$_{5/2}$
1397.2	2s^{2}2p ^{2}P$_{1/2}$–2s2p^2 ^{4}P$_{3/2}$
1399.7	2s^{2}2p ^{2}P$_{1/2}$–2s2p^2 ^{4}P$_{1/2}$
1401.1	2s^{2}2p ^{2}P$_{3/2}$–2s2p^2 ^{4}P$_{5/2}$
1404.7	2s^{2}2p ^{2}P$_{3/2}$–2s2p^2 ^{4}P$_{3/2}$
1407.3	2s^{2}2p ^{2}P$_{3/2}$–2s2p^2 ^{4}P$_{1/2}$

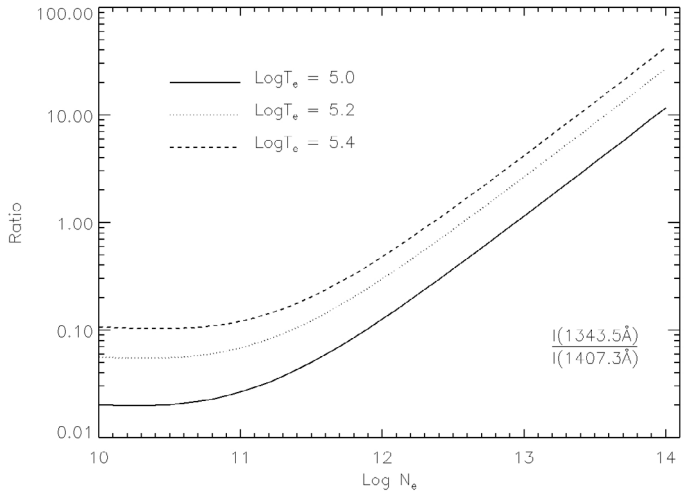

Fig. 5. Same as Fig. 3, but for the I(1343.5 Å)/I(1407.3 Å) ratio.

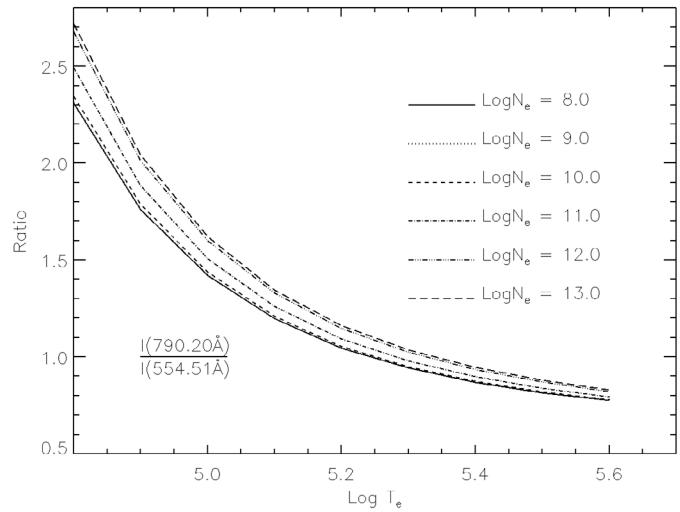

Fig. 6. The I(790.20 Å)/I(554.51 Å) line intensity ratio in O IV, where I is in energy units, plotted as a function of logarithmic electron temperature (T_e in K) at logarithmic electron densities (N_e in cm^{-3}) of log N_e = 8–13.

log $N_e = 12.5$ at the temperature of maximum fractional abundance for O IV in ionization equilibrium, $T_e = 10^{5.2}$ K (Bryans et al. 2009). These are consistent with the values of log $N_e \simeq 12.3$ determined for high density flares using extreme-ultraviolet lines of O V, formed at a similar temperature to O IV (Keenan et al. 1991).

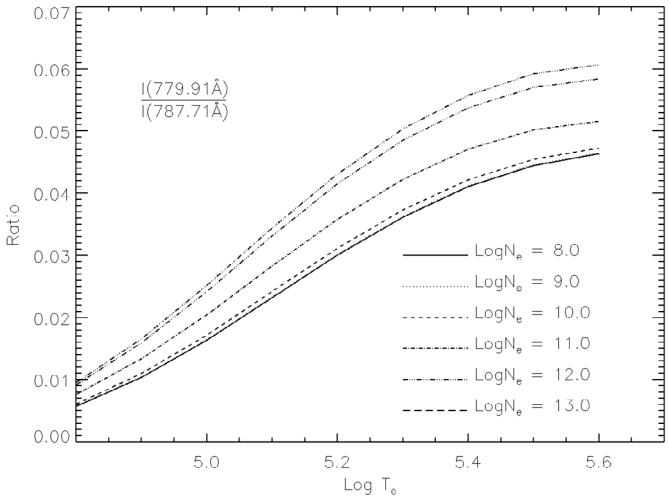

Fig. 7. Same as Fig. 6, but for the I(779.91 Å)/I(787.71 Å) ratio.

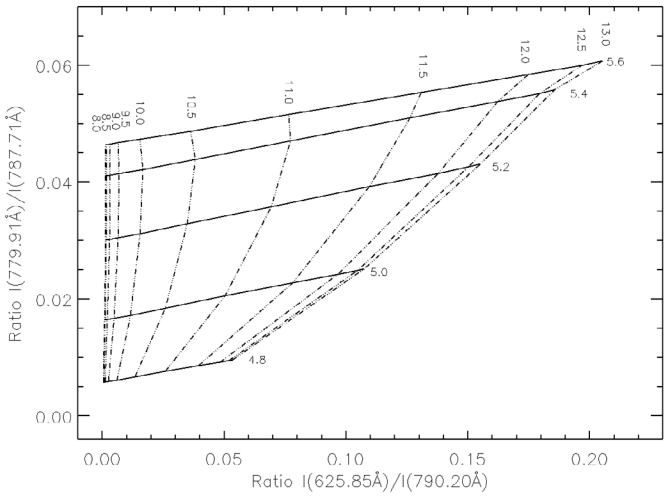

Fig. 8. Plot of the O IV line intensity ratio I(779.91 Å)/I(787.71 Å) against I(625.85 Å)/I(790.20 Å), where I is in energy units, for logarithmic electron temperatures (T_e in K) of log T_e = 4.8−5.6, and logarithmic electron densities (N_e in cm^{-3}) of log N_e = 8−13.

For temperature diagnostics, Flower & Nussbaumer (1975) have shown that the intensity ratio of lines within the $2s^22p\ ^2P$–$2s2p^2\ ^2D$ multiplet at ∼790 Å to those in $2s^22p\ ^2P$–$2s2p^2\ ^2P$ at ∼554 Å allows T_e to be estimated for the O IV emitting region of a plasma. This is shown in Fig. 6, where we plot the R_7 = I(790.20 Å)/I(554.51 Å) ratio as a function of T_e and N_e. Similarly, Curdt et al. (1997) have noted that the R_8 = I(779.91 Å)/I(787.71 Å) ratio is a T_e-diagnostic, and this is plotted in Fig. 7. An inspection of the two figures reveals that R_7 is in principle a better temperature diagnostic than R_8, as it is less sensitive to the adopted value of N_e. However, the emission lines in R_8 are much closer in wavelength and hence the ratio is more likely to be reliably measured. Indeed, Curdt et al. have determined R_8 = 0.033 from a SOHO/SUMER spectrum of the solar disk, which indicates $T_e \simeq 10^{5.1}$–$10^{5.3}$ K from Fig. 7 (the exact value depending on the adopted density), in good agreement with the temperature of maximum fractional abundance in ionization equilibrium for O IV, $T_e = 10^{5.2}$ K (Bryans et al. 2009). Unfortunately, to our knowledge, the R_7 ratio has not been measured due to the low spectral resolution of existing solar observations spanning the 554−790 Å wavelength range. However, O'Shea et al. (1996) have determined values of the multiplet intensity ratio I(790 Å)/I(554 Å) for several solar features from spectra obtained with the S-055 spectrometer on Skylab. These measurements lie in the range 0.47−0.56, and imply temperatures within ∼0.2 dex of that of maximum fractional abundance for O IV.

Under solar plasma conditions, O IV extreme-ultraviolet line ratios containing a component of the $2s2p^2\ ^4P$–$2p^3\ ^4S$ multiplet at ∼625 Å are strongly density sensitive (O'Shea et al. 1996). Unfortunately, in existing solar spectra the transitions – which lie at wavelengths of 624.62, 625.13 and 625.85 Å – are all blended with the strong Mg X resonance line at 624.94 Å. However, if the O IV features could be resolved, then in conjunction with other relatively nearby O IV lines they would allow the temperature *and* density of the O IV emitting region of a plasma to be simultaneously determined via ratio – ratio diagrams, as illustrated in Fig. 8.

In summary, we see that ultraviolet and extreme-ultraviolet emission lines of O IV provide a diverse portfolio of T_e and N_e diagnostics, applicable to a wide variety of astronomical sources ranging from gaseous nebulae to high electron density stellar flares. The present line ratio calculations, which include the most up-to-date atomic physics data, show good agreement with observations where available, hence providing support for their accuracy. However, higher spectral resolution observations of several O IV lines, such as the components of the $2s2p^2\ ^4P$–$2p^3\ ^4S$ multiplet at ∼625 Å, would be very useful to allow their intensities to be reliably measured and employed as diagnostics.

Acknowledgements. This work has been financed by the Science and Technology Facilities Council and Engineering and Physical Sciences Research Council of the United Kingdom, while P.J.C. and D.B.J. are grateful to the Department of Education and Learning (Northern Ireland) for the award of studentships. F.P.K. is grateful to AWE Aldermaston for the award of a William Penney Fellowship.

References

Aggarwal, K. M., & Keenan, F. P. 2008, A&A, 486, 1053
Blair, W. P., Long, K. S., Vancura, O., et al. 1991, ApJ, 379, L33
Brage, T., Judge, P. G., & Brekke, P. 1996, ApJ, 464, 1030
Bryans, P., Landi, E., & Savin, D. W. 2009, ApJ, submitted
Christian, D. J., Mathioudakis, M., Bloomfield, D. S., Dupuis, J., & Keenan, F. P. 2004, ApJ, 612, 1140
Cook, J. W., Keenan, F. P., & Bhatia, A. K. 1994, ApJ, 425, 861
Corrégé, G., & Hibbert, A. 2002, J. Phys. B, 35, 1211
Corrégé, G., & Hibbert, A. 2004, ADNDT, 86, 19
Curdt, W., Feldman, U., Laming, J. M., et al. 1997, A&AS, 126, 281
Dufton, P. L. 1977, Comput. Phys. Commun., 13, 25
Feibelman, W. A. 1997, ApJS, 112, 193
Feldman, U., & Doschek, G. A. 1978, ApJS, 37, 443
Flower, D. R., & Nussbaumer, H. 1975, A&A, 45, 145
Foster, V. J., Keenan, F. P., & Reid, R. H. G. 1996, A&A, 308, 1009
Foster, V. J., Reid, R. H. G., & Keenan, F. P. 1997, MNRAS, 288, 973
Galavís, M. E., Mendoza, C., & Zeippen, C. J. 1998, A&AS, 131, 499
Kastner, S. O., & Bhatia, A. K. 1984, JQSRT, 32, 249
Keenan, F. P., Dufton, P. L., Harra, L. K., et al. 1991, ApJ, 382, 349
Keenan, F. P., Conlon, E. S., Bowden, D. A., Feibelman, W. A., & Pradhan, A. K. 1993, ApJS, 88, 169
Keenan, F. P., Harra, L. K., Doschek, G. A., & Cook, J. W. 1994, ApJ, 432, 806
Keenan, F. P., McKenna, F. C., Bell, K. L., et al. 1997, ApJ, 487, 457
Keenan, F. P., Aller, L. H., Bell, K. L., et al. 1998, MNRAS, 295, 683
Keenan, F. P., Ahmed, S., Brage, T., et al. 2002, MNRAS, 337, 901
O'Shea, E., Foster, V. J., Keenan, F. P., et al. 1996, A&A, 306, 621
Sandlin, G. D., Bartoe, J.-D. F., Brueckner, G. E., Tousey, R., & VanHoosier, M. E. 1986, ApJS, 61, 801
Seaton, M. J. 1964, MNRAS, 127, 191
Tachiev, G., & Frose-Fischer, C. 2000, J. Phys. B, 33, 2419
Tayal, S. S. 2006, ApJS, 166, 634
Zhang, H. L., Graziani, M., & Pradhan, A. K. 1994, A&A, 283, 319